

**Error Probability for Direct-  
Sequence Spread-Spectrum  
Multiple-Access Communications  
Over Nonselective and Frequency-  
Selective Rician Fading Channels**

by

**Evangelos Geraniotis**

---

# Report Documentation Page

Form Approved  
OMB No. 0704-0188

Public reporting burden for the collection of information is estimated to average 1 hour per response, including the time for reviewing instructions, searching existing data sources, gathering and maintaining the data needed, and completing and reviewing the collection of information. Send comments regarding this burden estimate or any other aspect of this collection of information, including suggestions for reducing this burden, to Washington Headquarters Services, Directorate for Information Operations and Reports, 1215 Jefferson Davis Highway, Suite 1204, Arlington VA 22202-4302. Respondents should be aware that notwithstanding any other provision of law, no person shall be subject to a penalty for failing to comply with a collection of information if it does not display a currently valid OMB control number.

1. REPORT DATE <b>1986</b>		2. REPORT TYPE		3. DATES COVERED <b>00-00-1986 to 00-00-1986</b>	
4. TITLE AND SUBTITLE <b>Error Probability for Direct-Sequence Spread-Spectrum Multiple-Access Communications Over Nonselective and Frequency-Selective Rician Fading Channels</b>				5a. CONTRACT NUMBER	
				5b. GRANT NUMBER	
				5c. PROGRAM ELEMENT NUMBER	
6. AUTHOR(S)				5d. PROJECT NUMBER	
				5e. TASK NUMBER	
				5f. WORK UNIT NUMBER	
7. PERFORMING ORGANIZATION NAME(S) AND ADDRESS(ES) <b>University of Maryland, Electrical Engineering Department, College Park, MD, 20742</b>				8. PERFORMING ORGANIZATION REPORT NUMBER	
9. SPONSORING/MONITORING AGENCY NAME(S) AND ADDRESS(ES)				10. SPONSOR/MONITOR'S ACRONYM(S)	
				11. SPONSOR/MONITOR'S REPORT NUMBER(S)	
12. DISTRIBUTION/AVAILABILITY STATEMENT <b>Approved for public release; distribution unlimited</b>					
13. SUPPLEMENTARY NOTES					
14. ABSTRACT <b>see report</b>					
15. SUBJECT TERMS					
16. SECURITY CLASSIFICATION OF:			17. LIMITATION OF ABSTRACT	18. NUMBER OF PAGES <b>34</b>	19a. NAME OF RESPONSIBLE PERSON
a. REPORT <b>unclassified</b>	b. ABSTRACT <b>unclassified</b>	c. THIS PAGE <b>unclassified</b>			

**ERROR PROBABILITY FOR DIRECT-SEQUENCE SPREAD-SPECTRUM  
MULTIPLE-ACCESS COMMUNICATIONS OVER NONSELECTIVE AND  
FREQUENCY-SELECTIVE RICIAN FADING CHANNELS**

Evangelos Geraniotis, Member IEEE

Electrical Engineering Department  
and Systems Research Center  
University of Maryland  
College Park, MD 20742

**ABSTRACT**

An accurate approximation is obtained for the average probability of error in an asynchronous binary direct-sequence spread-spectrum multiple-access communications system operating over nonselective and frequency-selective Rician fading channels. The approximation is based on the integration of the characteristic function of the multiple-access interference which now consists of specular and scatter components. For nonselective fading the amount of computation required to evaluate this approximation grows linearly with the product  $KN$ , where  $K$  is the number of simultaneous transmitters and  $N$  is the number of chips per bit. For frequency-selective fading the computational effort grows linearly with the product  $KN^2$ . The resulting probability of error is also compared with an approximation based on the signal-to-noise ratio. Numerical results are presented for specific chip waveforms and signature sequences.

## I. INTRODUCTION

This paper is concerned with the average probability of error for asynchronous binary direct-sequence spread-spectrum multiple-access (DS/SSMA) communications over nonselective and frequency-selective Rician fading channels. The results presented represent a generalization of the analysis of [7] which considered only additive white Gaussian noise (AWGN) channels.

The system model is described in detail in [6]. Throughout this paper we restrict attention to binary DS/SSMA systems with phase-shift-keyed (PSK) modulation and chip waveforms which are pulses of arbitrary shape with duration equal to the inverse of the chip rate. However our results can be extended (using the results of [7]) to include other forms of direct-sequence modulation like quadriphase-shift-keying (QPSK), offset QPSK, and minimum-shift-keying (MSK).

The channel model considered in this paper is the Rician or specular-plus-Rayleigh fading channel model described in [1] for nonselective fading, and in [5] for selective fading. In the second case the fading is assumed to be frequency-selective [3]. Although our results can be extended to time-selective, as well as doubly-selective wide-sense-stationary uncorrelated-scattering (WSSUS) fading channels ([2], [5]), we restrict attention to frequency-selective channels, since these channels often arise in practice and, as shown in [5], single user DS/spread-spectrum systems outperform biphase PSK systems over such channels.

In [5] the average signal-to-noise ratio at the output of the receiver of a binary DS/SSMA system operating over time and frequency-selective Rician fading channels was evaluated. In [4] the moment space bounding

technique of [12] was applied to bound the probability of error of such systems. However the results were limited because of unsurpassable difficulties in evaluating high order moments of the interference. For the same reason, the approximation based on the Gauss Quadrature Rule, which was used in [10] - [11] for DS/SSMA systems over AWGN channels, is not computationally attractive in this case, since it requires calculation of moments which involve high order channel autocovariance functions that may not be measurable or otherwise available. Similarly, the bounds of [13] were based on convexity properties of the complementary error function which are valid only in the AWGN case. Finally, the results for two users of [14] for nonselective fading channels and [15] for time-selective fading channels appear difficult to extend so that they provide an efficient and accurate computational method for the multi-user case.

In this paper we obtain an approximation with a computational requirement which for nonselective fading is linear in the product  $KN$  and for frequency-selective fading is linear in the product  $KN^2$ , where  $K$  is the number of simultaneous transmitters and  $N$  is the number of chips per bit. This approximation is based on the integration of the characteristic function of the multiple-access interference component of the output of the correlation receiver. This component consists now of a fixed (or specular) part and a random (or scatter) part. This method, which we refer to as the characteristic-function method, was applied to DS/SSMA systems in [7] and DS/SS systems with specular multipath fading in [9] where it was shown to provide very accurate approximations to the average probability of error. Moreover, as shown in [8], any prespecified degree of accuracy can be achieved by using this approximation to obtain an expansion point for a

Taylor series representation of the actual probability of error. In the selective fading case, however, it is computationally untractable to evaluate the moments of the interference required for the series expansion method, therefore, in the sequel we consider only the characteristic-function method.

We should also point out at this point that the DS/SSMA system under consideration employs conventional matched filter receivers <sup>to</sup> combat rather than utilize the interference (multiple-access faded and nonfaded components) by discriminating against it. This is in contrast to the work of [17] - [18] where diversity reception is used to combine the contributions of the faded (reflected in those cases) paths and use them in the binary decision.

This paper is organized as follows. Nonselective Rician channels are considered in Section II, and frequency-selective Rician channels are treated in Section III. In each of these sections the fading channel model is first presented. Next the characteristic-function method is applied to each particular model and the computational requirements are considered. Finally a simpler approximation which is based on the average signal-to-noise ratio is cited for the sake of comparison. In Section IV numerical results are presented for specific chip waveforms and signature sequences.

## II. PERFORMANCE OF DS/SSMA COMMUNICATIONS OVER NONSELECTIVE RICIAN FADING CHANNELS

### A. A System and Channel Model

The system model is described in detail in [6] and [9]. Here we repeat the basic elements of this model so that the concepts and notation which are necessary for the rest of the paper are introduced.

The  $k$ -th transmitted signal for a binary DS/SSMA system with PSK modulation and arbitrary chip waveform can be expressed as

$$s_k(t) = \text{Re} \{ x_k(t) \exp(j2\pi f_c t) \} \quad (1)$$

where  $\text{Re}$  stands for real part,  $j = \sqrt{-1}$ ,  $f_c$  is the common carrier frequency, and the DS-spreaded signal  $x_k(t)$  is given by

$$x_k(t) = \sqrt{2P} b_k(t) \Psi(t) a_k(t) \exp(j\theta_k). \quad (2)$$

In (2)  $P$  is the power in each of the  $K$  transmitted signals; the equal power assumption is made for convenience in presenting numerical results, it is not necessary for the methods considered in this paper. The phase angle  $\theta_k$  introduced by the modulator is uniformly distributed in  $[0, 2\pi]$ . The shaping waveform  $\Psi(t)$  that appears in (2) is periodic with period  $T_c$  (the duration of a chip), it is defined by  $\Psi(t) = \psi(s)$  for  $s = t \pmod{T_c}$  where  $\psi(s)$  is a chip waveform of arbitrary shape (see [6] and [9]) which satisfies a time-limiting constraint and an average energy constraint. The data signal  $b_k(t)$  consists of rectangular pulses of duration  $T$  which take values  $+1$  and  $-1$  with equal probability. The  $\ell$ -th pulse has amplitude  $b_\ell^{(k)}$ . The information sequence  $(b_\ell^{(k)})$  is modeled as an i.i.d. sequence. The code waveform  $a_k(t)$  is a periodic sequence of rectangular pulses of amplitude  $+1$  or  $-1$  and duration  $T_c$ . The  $j$ -th code pulse has amplitude  $a_j^{(k)}$ . We assume that there are  $N$  code pulses in each data pulse ( $T = NT_c$ ) and that the period of the signature sequence  $(a_j^{(k)})$  is  $N$ .

For a system with  $K$  asynchronous simultaneous transmitted signals, the received signal at a receiver which is <sup>interested</sup> in the  $i$ -th signal is given by,

$$r(t) = \sum_{k=1}^K y_k(t - \tau_k) + n(t) \quad (3)$$

In (3)  $\tau_k$  is the time delay for the communication link between the  $k$ -th transmitter and the  $i$ -th receiver. The process  $n(t)$  is a white Gaussian noise process with two-sided spectral density  $N_0/2$ . Finally,  $y_k(t)$  is the fading channel output to input  $s_k(t)$ .

A Rician nonselective fading channel is described by the following input-output relationship

$$y_k(t) = s_k(t) + \text{Re} \{ \gamma_k A_\ell^{(k)} \exp(j\theta_\ell^{(k)}) x_k(t) \exp(j2\pi f_c t) \} \quad (4)$$

for  $\ell T \leq t < (\ell + 1)T$ . In (4)  $\gamma_k$  is a nonnegative real number and the nonnegative random variable  $A_\ell^{(k)}$  satisfies the normalization constraint

$$E \{ [A_\ell^{(k)}]^2 \} = 1. \quad (5)$$

The attenuation of the signal strength due to the fading during the time interval  $[\ell T, (\ell + 1)T)$  is thus represented by  $\gamma_k A_\ell^{(k)}$ , and the phase shift due to the fading is denoted by  $\theta_\ell^{(k)}$ . Therefore, for  $\gamma_k > 0$  the output signal is the sum of a nonfaded version of the input signal (specular component) and a nondelayed faded version of the input signal (scatter component). For  $A_\ell^{(k)}$  Rayleigh distributed and  $\theta_\ell^{(k)}$  uniformly distributed in  $[0, 2\pi]$  this model is discussed in [1]. Notice that from (4) and (3) the channel model reduces to the AWGN model if  $\gamma_k = 0$ . Similarly for  $\gamma_k \rightarrow \infty$  (very weak specular component in comparison to the faded component) the channel reduces to the Rayleigh nonselective channel.

Regarding the statistical dependence of the attenuation in different data bit intervals, we will consider the cases: (i)  $A_\ell^{(k)} = A_m^{(k)}$  for several values

of adjacent  $\ell$  and  $m$  (the length of the burst is immaterial for our analysis as long as it is longer than three adjacent bits) and (ii)  $A_\ell^{(k)}$  and  $A_m^{(k)}$  are independent if  $\ell \neq m$ . Case (i) corresponds to a system with no interleaving (or partial interleaving) and a channel with fading statistics which remain invariant over the duration of several data bits. An example of case (ii) arises in a system which is fully-interleaved or a fast fading channel. Similar restrictions are imposed on the phase sequence  $(\theta_\ell^{(k)})$ .

The  $i$ -th receiver is matched to the  $i$ -th transmitter signal; it is assumed capable of acquiring time and phase synchronization (coherent demodulation) with the nonfaded component of the  $i$ -th signal. Therefore, we may measure time delays and phase angles relative to  $\tau_i$  and  $\theta_i$ , respectively, and thus set  $\tau_i = \theta_i = 0$ . If there is not a nonfaded component we assume that the phase of the faded component of the Rician nonselective fading channel [see (3)] changes very slowly so that the receiver can again acquire time and phase synchronization. In this case we should let  $\theta_i + \theta_0^{(i)} = 0$ .

Once time and phase acquisition is completed the received signal is passed through a correlation receiver which outputs

$$Z_i = \int_0^T r(t)\psi(t)a_i(t) \cos(2\pi f_c t) dt. \quad (6)$$

If  $Z_i$  is positive the receiver will decide that a 1 was sent, otherwise it will output a -1. In practical spread-spectrum systems, the common carrier frequency  $f_c$  and bit duration  $T$  are such that  $f_c \gg T^{-1}$ ; consequently, the double-frequency terms in the integrand of (6) may be ignored.

Finally, concerning the interaction among the different communication links between the users, we may measure the delays  $\tau_k$  <sup>with</sup> respect to  $\tau_i$ , set  $\tau_i = 0$ , and assume that for  $k \neq i$   $\tau_k \pmod{T}$  is uniformly distributed in  $[0, T]$ . Then the

delays  $\tau_k$ , the phase angles  $\theta_k$ , and the data streams  $(b_\ell^{(k)})$  are assumed to be mutually independent for a given  $k$ , as well as for any two different transmitters. Finally, we assume that all communication links fade independently; therefore, all the random variables and/or random processes which characterize the fading are independent for any two different links.

### B. Evaluation of Error Probability via the Characteristic-Function Method

By ignoring the double-frequency terms in (6) we may write  $Z_i$  as

$$Z_i = (1/2 E_b T)^{1/2} (b_0^{(i)} + \eta_i + \bar{I}_i), \quad (7)$$

In (7)  $E_b \triangleq PT$  is the received energy per bit for the nonfaded component, the first term inside the parenthesis is the desired signal component (i.e., the  $i$ -th information signal for  $0 \leq t < T$ ),  $\eta_i$  represents the normalized contribution of the AWGN and of the faded component of the  $i$ -th signal, and  $\bar{I}_i$  stands for the normalized multiple-access interference (which now has nonfaded and faded components) due to all the other users besides the  $i$ -th user. We actually have that

$$\eta_i = \eta + \gamma_i F_i \quad (8)$$

and

$$\bar{I}_i = \sum_{k \neq i} (I_{k,i} + \gamma_k F_{k,i}), \quad (9)$$

where  $\eta$  is a zero-mean Gaussian random variable with variance  $N_0/2E_b$ ,  $F_i$  is the normalized interference due to the faded component of the  $i$ -th signal,  $I_{k,i}$  and  $F_{k,i}$  represent normalized interference due to the nonfaded and faded components of the  $k$ -th ( $k \neq i$ ) signal.

Due to the additive form of the multiple-access interference [see (9)], the characteristic-function method is recommended for the evaluation of the probability of error for the DS/SSMA systems under consideration. As in [7] we can write  $\bar{P}_{e,i}$ , the average probability of error for the  $i$ -th

receiver (the average to be considered with respect to all the random variables introduced by the transmitters and the channel) as

$$\begin{aligned}\bar{P}_{e,i} &= 1/2 P\{Z_i \leq 0 | b_0^{(i)} = +1\} + 1/2 P\{Z_i > 0 | b_0^{(i)} = -1\} \\ &= 1/2 - 1/2 P\{-1 < \eta_i + \bar{I}_i \leq 1\}.\end{aligned}\quad (10)$$

where  $\eta_i$  and  $\bar{I}_i$  were defined above. Let  $\phi_{\eta_i}$  and  $\phi_i$  denote the characteristic functions of the random variables of  $\eta_i$  and  $\bar{I}_i$ , respectively.

Since the distributions of  $\eta_i$  and  $\bar{I}_i$  considered in this paper are symmetric, the characteristic functions  $\phi_{\eta_i}$  and  $\phi_i$  are real-valued even functions.

Therefore as in [7] - [9] we can write

$$\bar{P}_{e,i} = \bar{P}_{e,i}^0 + \pi^{-1} \int_0^\infty u^{-1} (\sin u) \phi_{\eta_i}(u) [1 - \phi_i(u)] du \quad (11)$$

where  $\bar{P}_{e,i}^0$  is the average probability of error in the absence of multiple-access interference (i.e., when  $\bar{I}_i = 0$  or  $K = 1$ ). Because of (9) and the independence assumptions of Section II.A above we can write for each real  $u$

$$\phi_i(u) = \prod_{k \neq i} E\{\exp[ju(I_{k,i} + \gamma_k F_{k,i})]\}, \quad (12)$$

which facilitates the computation of the characteristic function of the multiple-access interference.

For the Rician nonselective fading channel of Section II.A we can easily derive that

$$F_i = b_0^{(i)} A_0^{(i)} \cos(\theta_0^{(i)}), \quad (13a)$$

$$I_{k,i} = T^{-1} [b_1^{(k)} R_{k,i}(\tau_k) + b_2^{(k)} \hat{R}_{k,i}(\tau_k)] \cos \theta_k', \quad (13b)$$

and

$$\begin{aligned}F_{k,i} &= T^{-1} [b_1^{(k)} A_1^{(k)} R_{k,i}(\tau_k) \cos(\theta_k' + \theta_1^{(k)}) \\ &\quad + b_2^{(k)} A_2^{(k)} \hat{R}_{k,i}(\tau_k) \cos(\theta_k' + \theta_2^{(k)})],\end{aligned}\quad (13c)$$

where

$$\theta_k' = \theta_k - 2\pi f_c \tau_k.$$

Recall that  $\tau_i = \theta_i = 0$  so that  $\theta_i' = 0$ . The arguments of the partial continuous crosscorrelation functions  $R_{k,i}$  and  $\hat{R}_{k,i}$  (defined in [6]) should be considered modulo  $T$ . Let  $\underline{b}_{-k} = (b_1^{(k)}, b_2^{(k)})$  denote the pair of the  $(\lambda_k - 1)$ -th and  $\lambda_k$ -th consecutive data bits (suppose that for  $k \neq i$   $\lambda_k T \leq \tau_k < (\lambda_k + 1)T$ ). If, for simplicity, we assume that the  $A_\ell^{(k)}$ 's are Rayleigh distributed in  $[0, 2\pi]$ , then since  $\theta_k' + \theta_\ell^{(k)} \pmod{2\pi}$  is also uniformly distributed in  $[0, 2\pi]$  the random variables  $F_i$  and  $F_{k,i}$  are conditionally zero-mean Gaussian when conditioned on  $b_0^{(i)}$  and  $(\underline{b}_{-k}, \tau_k)$ , respectively.

Next we proceed to the evaluation of the characteristic functions of  $\eta_i$  and  $\underline{I}_i$  which are necessary for the computation in (11). Let  $\sigma_i^2$  denote the variance of  $\eta_i$  defined by (8), then

$$\sigma_i^2 = (2E_b/N_0)^{-1} + 1/2\gamma_i^2, \quad (14)$$

$$P_{e,i}^0 = Q(\sigma_i^{-1}), \quad (15)$$

where  $Q$  is the complementary error function, and

$$\phi_{\eta_i}(u) = \exp(-1/2u^2\sigma_i^2). \quad (16)$$

To proceed further we need to evaluate the variance of the conditionally Gaussian random variable  $F_{k,i}$  given by (13c). It turns

out that for (i) constant fading

$$\text{Var}\{F_{k,i} | \underline{b}_{-k}, \tau_k\} = 1/2 T^{-2} [b_1^{(k)} R_{k,i}(\tau_k) + b_2^{(k)} \hat{R}_{k,i}(\tau_k)]^2, \quad (17)$$

and for (ii) independent fading

$$\text{Var}\{F_{k,i} | \tau_k\} = 1/2 T^{-2} \{R_{k,i}^2(\tau_k) + \hat{R}_{k,i}^2(\tau_k)\}. \quad (18)$$

For  $\ell T_c \leq \tau < (\ell+1)T_c$  and any arbitrary function  $h$  define

$$\sigma^2(\ell, h, \tau) = 1/2 T^{-2} [h(\ell+1)R_\psi(\tau) + h(\ell)\hat{R}_\psi(\tau)]^2, \quad (19)$$

$$\sigma_{k,i}^2(\ell; \tau) = 1/2 T^{-2} [R_{k,i}^2(\tau) + \hat{R}_{k,i}^2(\tau)], \quad (20)$$

and

$$\tilde{f}(u; \ell, h; \tau) = \frac{2}{\pi} \int_0^{\pi/2} \cos\left\{\frac{u}{T}[h(\ell+1)R_\psi(\tau) + h(\ell)\hat{R}_\psi(\tau)]\cos\theta\right\}d\theta. \quad (21)$$

In (19) and (21)  $R_\psi$  and  $\hat{R}_\psi$  are the continuous partial autocorrelation functions of the chip waveform. The functions  $R_{k,i}$  and  $\hat{R}_{k,i}$  depend on them and on the discrete crosscorrelation function of the  $k$ -th and  $i$ -th signature sequences  $C_{k,i}$ . Then after some straightforward but cumbersome manipulations, (12) becomes

$$\begin{aligned} \phi_i(u) = \prod_{k \neq i} \{ & (2N)^{-1} \sum_{\ell=0}^{N-1} T_c^{-1} \int_0^{T_c} \{\tilde{f}(u; \ell, \theta_{k,i}; \tau) \exp[-1/2u^2 \gamma_k^2 \sigma^2(\ell, \theta_{k,i}; \tau)] \\ & + \tilde{f}(u; \ell, \hat{\theta}_{k,i}; \tau) \exp[-1/2u^2 \gamma_k^2 \sigma^2(\ell, \hat{\theta}_{k,i}; \tau)] d\tau \} \end{aligned} \quad (22a)$$

for (i) constant fading, and

$$\begin{aligned} \phi_i(u) = \prod_{k \neq i} \{ & (2N)^{-1} \sum_{\ell=0}^{N-1} T_c^{-1} \int_0^{T_c} [\tilde{f}(u; \ell, \theta_{k,i}; \tau) + \tilde{f}(u; \ell, \hat{\theta}_{k,i}; \tau)] \\ & \cdot \exp[-1/2u^2 \gamma_k^2 \sigma_{k,i}^2(\ell; \tau)] d\tau \} \end{aligned} \quad (22b)$$

for (ii) independent fading.

If the channel encountered by the  $i$ -th transmitted signal is a Rayleigh nonselective fading channel (i.e., there is no non-faded component of the  $i$ -th signal) we need to modify the above results in the following way. We start with finite  $\gamma_i$  and define  $\bar{E}_b \stackrel{\Delta}{=} (1 + \gamma_i^2)PT$  to be the total received energy at the  $i$ -th receiver in the absence of AWGN and multiple-access interference (i.e.,  $K = 1$ ), and  $\bar{\gamma}_k = (1 + \gamma_k^2)/(1 + \gamma_i^2)$  to be the ratio of the total received energy from the  $k$ -th signal to the total received energy from the  $i$ -th signal. For large  $\gamma_i$ , we assume (see Section II.A) that the receiver acquires time and phase synchronization with the faded component of the  $i$ -th signal, so that we may set  $\theta_i + \theta_0^{(i)} = 0$  and together with the definitions above write (7) and (8) - (9) as

$$Z_i = (1/2\bar{E}_b T)^{1/2} \left[ \eta + \frac{1}{\sqrt{1+\gamma_i^2}} (b_0^{(i)} \cos \theta_i + \gamma_i b_0^{(i)} A_0^{(i)}) + \sum_{k \neq i} \frac{\bar{\gamma}_k}{\sqrt{1+\gamma_k^2}} (I_{k,i} + \gamma_k F_{k,i}) \right]. \quad (23)$$

If we fix  $\bar{E}_b$  and let  $\gamma_i \rightarrow \infty$  (23) reduces to

$$Z_i = (1/2\bar{E}_b T)^{1/2} [b_0^{(i)} A_0^{(i)} + \eta_i + \bar{I}_i] \quad (24)$$

where  $A_0^{(i)}$  is Rayleigh distributed (with second order moment 1),  $\eta_i = \eta$  is zero-mean Gaussian with variance  $N_0/2\bar{E}_b$ , and  $\bar{I}_i$  is given by

$$\bar{I}_i = \sum_{k \neq i} \frac{\bar{\gamma}_k}{\sqrt{1+\gamma_k^2}} (I_{k,i} + \gamma_k F_{k,i}) \quad (25)$$

where  $I_{k,i}$  and  $F_{k,i}$  are as defined in (13b) - (13c).

A discussion of the computational requirements for formulas of the type of (11) can be found in [7] - [8] and since the situation here is very similar with that treated there, it will not be repeated. However, it is worth observing that since there is a summation of  $N$  terms and a product of  $K$  terms in (22a) - (22b) the computational effort for this method grows linearly with the product  $KN$ .

Starting from (24) and proceeding as for (10), we find that  $P_{e,i}(A_0^{(i)})$  the conditional probability of error given  $A_0^{(i)}$  can be expressed initially as

$$P_{e,i}(A_0^{(i)}) = 1/2 - 1/2 P\{-A_0^{(i)} < \eta_i + \bar{I}_i \leq A_0^{(i)}\}, \quad (26)$$

and finally [cf. (11)] as

$$P_{e,i}(A_0^{(i)}) = P_{e,i}^0(A_0^{(i)}) + \pi^{-1} \int_0^\infty u^{-1} \sin(A_0^{(i)} u) \phi_{\eta_i}(u) [1 - \phi_i(u)] du. \quad (27)$$

Since  $\eta_i$  is now zero-mean Gaussian with variance

$$\sigma_i^2 = (2\bar{E}_b/N_0)^{-1} \quad (28)$$

$\phi_{\eta_i}(u)$  is given by (16) with  $\sigma_i^2$  defined by (28) and

$$P_{e,i}^0(A_0^{(i)}) = Q(A_0^{(i)}/\sigma_i). \quad (29)$$

To obtain the average probability of error  $\bar{P}_{e,i}$  we should average the second member of (27) with respect to the Rayleigh distributed random variable

$A_0^{(i)}$ . The result (see Appendix A of [9] for the proof) is

$$\bar{P}_{e,i} = P_{e,i}^0 + 1/2\pi^{-1/2} \int_0^\infty \exp(-1/4u^2)\phi_{\eta_i}(u)[1 - \phi_i(u)]du \quad (30)$$

where

$$P_{e,i}^0 = 1/2\{1 - [1 + (\bar{E}_b/N_0)^{-1}]^{-1/2}\} \quad (31)$$

and  $\phi_i(u)$  is given by (22a) and (23b) for case (i) constant fading and (ii)

independent fading, respectively, evaluated [because of (25)] at  $\bar{\gamma}_k u / \sqrt{1 + \bar{\gamma}_k^2}$  instead of  $u$ .

### C. Approximation Based on Average Signal-to-Noise Ratio

For the sake of comparison we next cite an approximation based on  $\text{SNR}_i$  the average signal-to-noise ratio at the output of the  $i$ -th receiver. As suggested in [6]

$$\text{SNR}_i \triangleq E\{Z_i\}/[\text{Var}\{Z_i\}]^{1/2} \quad (32)$$

which in our case becomes

$$\text{SNR}_i = [\text{Var}\{\eta_i\} + \sum_{k \neq i} \text{Var}(I_{k,i} + \gamma_{k,i} F_{k,i})]^{-1/2}. \quad (33)$$

For Rician nonselective fading (33) reduces to

$$\text{SNR}_i = \{(2\bar{E}_b/N_0)^{-1} + 1/2\bar{\gamma}_i^2 + \sum_{k \neq i} (1 + \bar{\gamma}_k^2) T^{-3} [\mu_{k,i}(0)m_\psi + \mu_{k,i}(1)m'_\psi]\}^{-1/2} \quad (34)$$

and the resulting approximation to the average error probability is

$$\bar{P}_{e,i}^G = Q(\text{SNR}_i). \quad (35)$$

In (34) the function  $\mu_{k,i}(n)$  (see [6]) depends on the discrete crosscorrelation function  $C_{k,i}$  while  $m_\psi$  and  $m'_\psi$  (again see [6]) depend on  $R_\psi$  and  $\hat{R}_\psi$ . For Rayleigh nonselective fading (33) becomes

$$\text{SNR}_i = \{(\bar{E}_b/N_0)^{-1} + \sum_{k \neq i} \bar{\gamma}_k^{-2} T^{-3} [\mu_{k,i}(0)m_\psi + \mu_{k,i}(1)m'_\psi]\}^{-1/2} \quad (36)$$

and the resulting approximation is

$$\bar{P}_{e,i}^G = 1/2\{1 - [1 + (\text{SNR}_i)^{-2}]^{-1/2}\}. \quad (37)$$

Notice that, in contrast to the approximation based on the characteristic-function method, the approximations obtained via the signal-to-noise ratio do not distinguish between the constant and independent fading cases considered in Section II.A.

### III. PERFORMANCE OF DS/SS COMMUNICATIONS OVER FREQUENCY-SELECTIVE RICIAN FADING CHANNELS

#### A. Channel Model

The input-output relationship for a wide-sense-stationary uncorrelated-scattering (WSSUS) frequency-selective fading channel can be expressed as

$$y_k(t) = s_k(t) + \text{Re}\{u_k(t-v_k T)\exp[j2\pi f_c(t-v_k T)]\} \quad (38)$$

where

$$u_k(t) = \gamma_k \int_{-\infty}^{\infty} h_k(t,\zeta)x_k(t-\zeta)d\zeta. \quad (39)$$

The fading process  $h_k(t,\zeta)$  (which can be thought of as the time-varying impulse response of a low pass filter) is a zero-mean complex Gaussian random process with autocovariance

$$E\{h_k(t,\zeta)h_k^*(s,\xi)\} = g_k(\zeta)\delta(\zeta-\xi), \quad (40a)$$

and satisfies the normalization constraint

$$\int_{-\infty}^{\infty} g_k(\zeta)d\zeta = 1, \quad (40b)$$

and the necessary condition for stationary bandpass processes (see [2], and the discussion in Section 2.2 of [4])

$$E\{h_k(t,\zeta)h_k(s,\xi)\} = 0. \quad (40c)$$

The first term of (38) is again termed the specular component while the second term in (38) is now called the diffuse faded component. If  $\gamma_k$  is a positive real number, the channel is a Rician fading channel. If  $\gamma_k \rightarrow \infty$  the faded component becomes dominant and the channel is a Rayleigh fading channel. This model is basically described in detail in [2] - [3], in particular the Rician fading channel is described in [4] - [5]. Here we consider a slightly more general model since for the Rician case we allow [see (38)] an average delay  $v_k T$  ( $v_k$  is a nonnegative integer) between the nonfaded specular component and the diffused faded component.

The WSSUS fading model can be thought of arising when the transmitted signal encounters a slowly-moving scattering random medium which can be modeled as a layered scatterer consisting of a large number of layers of infinitesimal thickness. It, is therefore, a frequency-selective channel, i.e., it is dispersive only in frequency. The high-frequency (HF) ionospheric and the microwave tropospheric scatter channels fit the above description; Section 2.1 of [4] provides more examples of such channels.

We impose a limitation on the selectivity of the channel in order to facilitate subsequent analysis. In particular, as in [5] and [3] it is assumed that

$$g_k(\zeta) = 0 \quad \text{for } |\zeta| > T \quad (41)$$

which is a constraint on the frequency selectivity of the channel that allows us to restrict attention to the intersymbol interference from the two adjacent data bits.

With regard to the average delay  $\nu_k T$  between the nonfaded specular component and the faded scatter component of  $y_k(t)$  in (38), we will consider the two extreme cases (i)  $\nu_k = 0$  (no delay) and (ii)  $\nu_k \geq 3$  (large delay). The choice of the integer 3 as the lower bound for  $\nu_k$  in (ii) is justified by the fact that, in view of (41), it uncorrelates the contributions of the nonfaded and faded components at the output of the receiver.

#### B. Evaluation of Error Probability via the Characteristic-Function Method

The output of the matched filter  $Z_i$  is again given by (7) where  $\eta_i$  and  $I_i$  are given by (8) and (9), respectively. The random variable  $\eta$  in (8) is again zero-mean Gaussian with variance  $N_0/2E_b$ ; the nonfaded component of the interference (due to the  $k$ -th signal)  $I_{k,i}$  is given by (13b), but the faded

components  $F_i$  and  $F_{k,i}$  of (8) - (9) are now found [combine (38) - (39) with, (3) and (6)] to be

$$F_i = \text{Re}\{\tilde{F}_i\}, \quad (42a)$$

$$\tilde{F}_i = T^{-1} \int_{-\infty}^{\infty} h_i(t-v_i T, \zeta) \Gamma_i(t, \zeta+v_i T) \exp(j\phi_i) d\zeta dt, \quad (42b)$$

$$F_{k,i} = \text{Re}\{\tilde{F}_{k,i}\}, \quad (42c)$$

$$\tilde{F}_{k,i} = T^{-1} \int_0^T \int_{-\infty}^{\infty} h_k(t-\tau_k-v_k T, \zeta) \Gamma_{k,i}(t, \zeta+\tau_k+v_k T) \exp(j\phi_k) d\zeta dt, \quad (42d)$$

where

$$\Gamma_{k,i}(t, \zeta) = a_k(t-\zeta) a_i(t) b_k(t-\zeta) b_i(t) \Psi(t-\zeta) \Psi(t)$$

and

$$\phi_k = \theta_k - 2\pi f_c (\tau_k + v_k T).$$

The function  $\Gamma_{i,i}$  is denoted by  $\Gamma_i$ . Since  $h_k$  is a complex Gaussian random field, the random variables  $F_i$  and  $F_{k,i}$  are conditionally Gaussian random variables (conditioned on time delays, phase angles, and data streams). Recall that  $v_k T$  ( $1 \leq k \leq K$ ) accounts for the average delay between the nonfaded and the diffused components of the channel output (see Section III.A)

Next, we proceed to the evaluation of the average error probability  $\bar{P}_{e,i}$  via the characteristic-function method. As in the nonselective fading case, we need to evaluate  $\bar{P}_{e,i}$ ,  $\phi_{\eta_i}$ , and  $\phi_i$  for use in (11). We follow the same steps as before. The random variable  $F_i$  is zero-mean conditionally Gaussian with conditional variance

$$\begin{aligned} \text{Var}\{F_i | \underline{b}'_i\} &= 1/2 E\{\tilde{F}_i \tilde{F}_i^*\} \\ &= T^{-2} \int_0^T g_i(\zeta) [R_i^2(\zeta) + \hat{R}_i^2(\zeta) + (b_{1'}^{(i)} + b_{2'}^{(i)}) R_i(\zeta) \hat{R}_i(\zeta)] d\zeta. \end{aligned} \quad (43)$$

where  $\underline{b}'_i = (b_{1'}^{(i)}, b_{2'}^{(i)})$  denotes the pair of the  $(v_i-1)$ -th and  $v_i$ -th consecutive data bits of the  $i$ -th data stream. To derive (43) we used

(42a), (42b), (40a) - (40c), and (41). The Gaussian random variable  $\eta_i$  has then conditional variance

$$\text{Var}\{\eta_i | \underline{b}'_i\} = (2E_b/N_0)^{-1} + \gamma_i^2 \text{Var}\{F_i | \underline{b}'_i\}. \quad (44)$$

Then, if we define

$$[\sigma_i^{(1)}]^2 = (2E_b/N_0)^{-1} + \gamma_i^2 \int_0^T g_i(\zeta) [R_i^2(\zeta) + \hat{R}_i^2(\zeta)] d\zeta \quad (45a)$$

$$[\sigma_i^{(2)}]^2 = (2E_b/N_0)^{-1} + \gamma_i^2 T^{-2} \int_0^T g_i(\zeta) [R_i(\zeta) + \hat{R}_i(\zeta)]^2 d\zeta \quad (45b)$$

$$[\sigma_i^{(3)}]^2 = (2E_b/N_0)^{-1} + \gamma_i^2 T^{-2} \int_0^T g_i(\zeta) [R_i(\zeta) - \hat{R}_i(\zeta)]^2 d\zeta, \quad (45c)$$

we can write

$$P_{e,i}^n = \sum_{j=1}^3 c_j Q([\sigma_i^{(j)}]^{-1}) \quad (46)$$

and

$$\phi_{\eta_i} = \sum_{j=1}^3 c_j \exp\{-1/2[u\sigma_i^{(j)}]^2\} \quad (47)$$

where  $c_1 = 1/2$  and  $c_2 = c_3 = 1/4$ . Note that these two results are independent of the events  $v_i = 0$  (no delay: case (i) of Section III.A or  $v_i \geq 3$  (large delay: case (ii) of Section III.A.

The next step is to evaluate  $\phi_i$  through (12) with  $I_{k,i}$  and  $F_{k,i}$  given by (13b) and (42c) - (42d), respectively. We first compute the conditional variance of  $F_{k,i}$ , this turns out to be

$$\begin{aligned} \text{Var}\{F_{k,i} | \underline{b}'_k, \tau\} = 1/2T^{-2} \{ & \int_0^\tau g_k(\zeta - \tau + T) [b_{1'}^{(k)} R_{k,i}(\zeta) + b_{2'}^{(k)} \hat{R}_{k,i}(\zeta)]^2 d\zeta \\ & + \int_0^T g_k(\zeta - \tau) [b_{2'}^{(k)} R_{k,i}(\zeta) + b_{3'}^{(k)} \hat{R}_{k,i}(\zeta)]^2 d\zeta \\ & + \int_\tau^T g_k(\zeta - \tau - T) [b_{3'}^{(k)} R_{k,i}(\zeta) + b_{4'}^{(k)} \hat{R}_{k,i}(\zeta)]^2 d\zeta \}. \end{aligned} \quad (48)$$

In (48)  $\underline{b}'_k = (b_{1'}^{(k)}, b_{2'}^{(k)}, b_{3'}^{(k)}, b_{4'}^{(k)})$  ( $k \neq i$ ) is the quadruple which consists of the  $(\mu_k - 2)$ -th,  $(\mu_k - 1)$ -th,  $\mu_k$ -th, and  $(\mu_k + 1)$ -th consecutive bits of the  $k$ -th data stream,  $\mu_k \stackrel{\Delta}{=} \lambda_k + v_k$ , and  $\tau = \tau_k \pmod T$  where

$\ell T_c \leq \tau < (\ell+1)T_c$ . The conditional variance about takes on 8 different values which we denote by  $[\sigma_{k,i}^{(j)}(\ell;\tau)]^2$  and  $[\hat{\sigma}_{k,i}^{(j)}(\ell;\tau)]^2$  for  $j = 1, 2, 3, 4$ .

Then the characteristic function  $\phi_i$  is derived as

$$\begin{aligned} \phi_i(u) = \prod_{k \neq i} \{ (8N)^{-1} \sum_{\ell=0}^{N-1} T_c^{-1} \int_0^{T_c} [\tilde{f}(u; \ell, \theta_{k,i}; \tau) \sum_{j=1}^4 \exp\{-1/2[uY_k \sigma_{k,i}^{(j)}(\ell;\tau)]^2\} \\ + \tilde{f}(u; \ell, \hat{\theta}_{k,i}; \tau) \sum_{j=1}^4 \exp\{-1/2[uY_k \hat{\sigma}_{k,i}^{(j)}(\ell;\tau)]^2\}] d\tau \} \end{aligned} \quad (49a)$$

for (i) no delay ( $v_k = 0$ , all  $k$ ), and

$$\begin{aligned} \phi_i(u) = \prod_{k \neq i} \{ (8N)^{-1} \sum_{\ell=0}^{N-1} T_c^{-1} \int_0^{T_c} [\tilde{f}(u; \ell, \theta_{k,i}; \tau) + \tilde{f}(u; \ell, \hat{\theta}_{k,i}; \tau)] \\ \cdot \sum_{j=1}^4 [\exp\{-1/2[uY_k \sigma_{k,i}^{(j)}(\ell;\tau)]^2\} \\ + \exp\{-1/2[uY_k \hat{\sigma}_{k,i}^{(j)}(\ell;\tau)]^2\}] d\tau \} \end{aligned} \quad (49b)$$

for (ii) large delay ( $v_k \geq 3$ , all  $k$ ). In case (i)  $I_{k,i}$  [given by (13b)] and  $F_{k,i}$  above are correlated [ $\underline{b}'_k = (b_1^{(k)}, b_k^{(k)}, b_4^{(k)})$ ]. In case (ii)  $I_{k,i}$  and  $F_{k,i}$  are uncorrelated ( $\underline{b}_k$  and  $\underline{b}'_k$  have no components in common). These facts are reflected in the form of  $\phi_i$  in (49a) and (49b) (the function  $\tilde{f}$  and the sum with the four terms are the characteristic functions of  $I_{k,i}$  and  $F_{k,i}$  given  $\tau$  respectively). The function  $\tilde{f}$  is as defined in (21).

To see on the computational effort grows linearly with  $KN^2$ , notice that in (49a) - (49b), besides the product of  $K-1$  terms and the summation of  $N$  terms, the integrals split into summations with a total of  $N$  terms as well [e.g.,  $\int_0^\tau = \sum_{n=0}^{\ell=1} \int_{nT_c}^{(n+1)T_c} + \int_{\ell T_c}^\tau$ , for  $\ell T_c \leq \tau < (\ell+1)T_c$ ].

#### C. Approximation Based on the Average Signal-to-Noise Ratio

The average signal-to-noise ratio in this case is given by [cf. (34)]

$$\text{SNR}_i = \{[\sigma_i^{(1)}]^2 + \sum_{k \neq i} (1+\gamma_k^2) [\mu_{k,i}^{(0)} m_\psi + \mu_{k,i}^{(1)} m'_\psi]\}^{-1/2} \quad (50)$$

where  $\sigma_i^{(1)}$  is given by (45a) above. This is a slight generalization of the results of [5] for arbitrary chip waveforms. Notice that  $\text{SNR}_i$  and the resulting approximation (35) cannot distinguish between cases (i) and (ii) (no delay versus large delay) of the fading model of Section III.A.

#### IV. NUMERICAL RESULTS AND CONCLUSIONS

All the signatures sequences employed in this section are AO/LSE m-sequences of lengths  $N=31$  and  $127$ . In particular, for a DS/SSMA system with  $K$  users the first  $K$  sequences of Figures A.1.(a) ( $N=31$ ) and A.1.(b) ( $N=127$ ) of [15] are used.

For  $\bar{P}_{e,i}$ , the approximation to the error probability which is based on the characteristic-function method, we use Simson's integration technique with the same parameters as in Section III of [7] ( $L=20$ ,  $\epsilon < 10^{-14}$ ,  $n_\theta = 10$ ,  $n_\tau = 10$ , and  $n = 20$ ). We set  $i=1$  and consider  $\bar{P}_{e,1}$  for the error probability of the receiver matched to the first signal.

First, we present numerical results for DS/SSMA systems with nonselective Rician and Rayleigh fading channels. In Table 1 the Gaussian approximation to the error probability  $\bar{P}_{e,1}^G$  and the approximations  $\bar{P}_{e,1}^{(i)}$  and  $\bar{P}_{e,1}^{(ii)}$  obtained by the characteristic-function method are compared for a DS/SSMA system with sequences of length 31 and  $K = 2, 3$ , and 4 simultaneous users. The communications link between the  $k$ -th transmitter and the receiver matched to the first signal is a Rician nonselective fading channel with relative power of the faded component  $\gamma_k^2 = \gamma^2 = .1$ ,  $1 \leq k \leq K$ . The error probabilities  $\bar{P}_{e,1}^{(i)}$  and  $\bar{P}_{e,1}^{(ii)}$  correspond to the cases of (i) slow fading and (ii) fast fading discussed in Section II.A. We observe that the Gaussian approximation is somewhat optimistic when compared with the more accurate approximations based on the characteristic function but still in good agreement with them. Notice that slow fading causes a slightly worse performance of the DS/SSMA system than fast fading. Recall that the Gaussian approximation results in the same value of the error probability for both slow and fast fading.

In Figure 1 we plotted both  $\bar{P}_{e,1}^{(i)}$  (for slow fading) and  $\bar{P}_{e,1}^G$  versus  $E_b/N_0$  for a DS/SSMA system with  $K=3$ ,  $N=31$ , and Rician nonselective fading. The relative power of all faded components are  $\gamma^2 = .01, .05, .1, .2, \text{ and } .4$ . Notice that as  $\gamma^2$  increases the system degrades gracefully. For a nonselective fading channels DS/SS modulation enables the matched filter receiver to discriminate effectively against the nonfaded and faded components of the interfering signals but not against the faded component of the desired signal. This explains why the error probability is already larger than  $10^{-3}$  for  $\gamma^2 = .1, .2, \text{ and } .4$ . Finally, notice that the accuracy of the Gaussian approximation improves as  $\gamma^2$  increases.

In Table 2 we compare the performance of DS/SSMA systems with rectangular and sine chip waveforms. The sine chip waveform used is  $\psi(t) = \sqrt{2} \sin(\pi t/T_c)$ ,  $0 \leq t \leq T_c$ . The system parameters are  $K=3$ , and  $N=31$ . The Rician nonselective slow fading channel parameter takes on the values  $\gamma^2 = .01$  and  $.1$ . For moderately heavy fading ( $\gamma^2 = .1$ ) the rectangular chip waveform results in a slightly better performance than the sine chip waveform as both the Gaussian approximation  $\bar{P}_{e,1}^G$  and the more accurate approximation  $\bar{P}_{e,1}^{(i)}$  indicate. For light fading ( $\gamma^2 = .01$ ) the Gaussian approximation still shows better performance for the sine chip waveform for all values of  $E_b/N_0$ ; however, the more accurate approximation indicates that the sine chip waveform outperforms the rectangular chip waveform only for low signal-to-noise ratios; the situation is reversed for higher signal-to-noise ratios.

In Table 3 we present results for a DS/SSMA system with  $K=3$ ,  $N=31$  and Rayleigh nonselective fading channels with relative power of faded components taking values  $\tilde{\gamma}^2 = .01, .1, \text{ and } .2$ . The system performance has now

degraded considerably and higher signal-to-noise ratios were considered. Notice that the Gaussian approximation is conservative and for large values of  $\bar{\gamma}^2$  is off the actual value by one order of magnitude. On the other hand the values of the accurate approximation for (i) slow fading and (ii) fast fading do not differ in the first four significant digits.

Next, we consider DS/SSMA systems operating through Rician frequency-selective channels. In Table 4 the Gaussian approximation is compared to the approximation obtained via the characteristic-function method for the cases (i) zero average delay between nonfaded and faded components and (ii) large delay (see Section III.A) and DS/SSMA systems with  $K=3$  and  $N=31$  and 127. The relative power of the diffuse component is  $\gamma^2=.4$  for all signals. Notice that the system performance for case (ii) gives slightly lower error probability than case (i) due to the more extensive randomization involved. The Gaussian approximation results in an optimistic estimate of the error probability for all cases but it is satisfactorily close to the more accurate results. Recall that the Gaussian approximation takes the same value for the aforementioned cases (i) and (ii).

In Figure 2  $\bar{P}_{e,1}^G$  and  $\bar{P}_{e,1}^{(i)}$  are plotted versus  $E_b/N_0$  for DS/SSMA systems with  $N=31$  and  $K=2, 3,$  and  $4$ . The autocovariance function of the frequency-selective WSSUS channel is triangular:  $g_k(\tau) = \frac{1}{T}(1 - \frac{|t|}{T})$  for  $|t| \leq T$  and 0 otherwise. The relative power of all the faded components is  $\gamma^2=.4$ . Notice that for an error probability of  $10^{-5}$  the Gaussian approximation is off by almost 1 dB for  $K=3$ . For fixed  $E_b/N_0$  the Gaussian approximation is satisfactory for all cases as it is also indicated by the results of Table 4.

Finally, in Figure 3 we have plotted  $\bar{P}_{e,1}^{(i)}$  versus  $E_b/N_0$  for a DS/SSMA system with  $K=3$  and  $N=31$  and relative power in the diffuse component taking values  $\gamma^2=0., .1, .2, .3,$  and  $.4$ . Notice the graceful degradation of the system performance as  $\gamma^2$  increases. The value  $\gamma^2=0.$  corresponds to DS/SSMA with an AWGN channel. A comparison of Figures 1 and 3 verifies that DS/SS modulation is much more efficient against frequency-selective fading than against nonselective fading.

## REFERENCES

- [1] G.L. Turin, "Communication through noisy, random-multipath channels," IRE National Convention Record. pt. 4, pp. 154-166, 1956.
- [2] P.A. Bello, "Characterization of randomly time-invariant linear channels," IEEE Transactions on Communication Systems, vol. CS-11, pp. 360-393, December 1963.
- [3] P.A. Bello and B.D. Nollin, "The influence of fading spectrum on the binary error probabilities of incoherent and differentially coherent matched filter receivers," IRE Transactions on Communication Systems, vol. CS-11, pp. 160-168, June 1962.
- [4] D.E. Borth, "Performance analysis of direct-sequence spread-spectrum multiple-access communication via fading channels," Ph.D. Thesis, Department of Electrical Engineering, University of Illinois (also Coordinated Science Laboratory Report R-880), April 1980.
- [5] D.E. Borth, and M.B. Pursley, "Analysis of direct-sequence spread-spectrum multiple-access communication over Rician fading channels," IEEE Transactions on Communications, vol. COM-27, pp. 1566-1577, October 1979.
- [6] M.B. Pursley, "Spread-spectrum multiple-access communications," in Multi-User Communication Systems, G. Longo (ed.), Springer-Verlag, Vienna and New York, pp. 139-199, 1981.
- [7] E.A. Geraniotis, and M.B. Pursley, "Error probability for direct-sequence spread-spectrum multiple-access communications -- Part II: Approximations," Special Issue on Spread-Spectrum Communications of the IEEE Transactions on Communications, vol. COM-30, pp. 985-995, May 1982.
- [8] E.A. Geraniotis and M.B. Pursley, "Error probability for binary PSK spread-spectrum multiple-access communications," Proceedings of the 1981 Conference on Information Sciences and Systems, Johns Hopkins University, pp. 238-244, March 1981.
- [9] E.A. Geraniotis and M.B. Pursley, "Performance of coherent direct-sequence spread-spectrum communications over specular multipath fading channels," IEEE Transactions on Communications, Vol. COM-33, pp. 502-508, June 1985.
- [10] K.-T. Wu, "Average error probability for DS-SSMA communications: The Gram-Charlier expansion approach," Proceedings of the Nineteenth Annual Allerton Conference on Communication, Control, and Computing, pp. 237-246, September 1981. [See also K.-T. Wu, "Direct sequence spread spectrum communications: applications to multiple-access and jamming resistance," Ph.D. Thesis, University of Michigan, 1981.]

- [11] D. Laforge et al., "Bit error rate evaluation for multiple-access spread-spectrum systems," IEEE Transactions on Communications, Vol. COM-32, pp. 660-669, June 1984.
- [12] K. Yao, "Error probability of asynchronous spread spectrum multiple access communication systems," IEEE Transactions on Communications, vol. COM-25, pp. 803-809, August 1977.
- [13] M.B. Pursley, D.V. Sarwate, and W.E. Stark, "Error probability for direct-sequence spread-spectrum multiple-access communications -- Part I: Upper and lower bounds," IEEE Transactions on Communications, vol. COM-30, pp. 975-984, May 1982.
- [14] R.C. Hanlon, C.S. Gardner, "Error performance of direct sequence spread spectrum systems on non-selective fading channels," IEEE Transactions on Communications, vol. COM-27, pp. 1696-1700, November 1979.
- [15] C.S. Gardner, and J.A. Orr, "Fading effects on the performance of a spread-spectrum multiple-access communication system," IEEE Transactions on Communications, vol. COM-27, pp. 143-149, January 1979.
- [16] M.B. Pursley and H.F.A. Roefs, "Numerical evaluation of correlation parameters for optimal phases of binary shift-register sequences," IEEE Transactions on Communications, vol. COM-27, 1597-1604, October 1979.
- [17] G. L. Turin, "Introduction to spread-spectrum anti-multipath techniques and their application to urban digital radio," Proceedings of the IEEE, Vol. 68, pp. 328-353, March 1980.
- [18] J. S. Lehnert and M. B. Pursley, "Multipath diversity reception of coherent direct-sequence spread-spectrum communications," Proceedings of the Conference on Information Sciences and Systems, Johns Hopkins Univ., pp.770-775, March 1983.

### Table Captions

- Table 1. Probability of error for DS/SSMA systems with Rician nonselective fading ( $N=31$ ,  $\gamma^2=.1$ ).
- Table 2. Probability of error for DS/SSMA systems with different chip waveforms and Rician nonselective fading ( $K=3$ ,  $N=31$ ).
- Table 3. Probability of error for a DS/SSMA system with Rayleigh nonselective fading ( $K=3$ ,  $N=31$ ).
- Table 4. Probability of error for a DS/SSMA system with frequency-selective fading ( $K=3$ ,  $\gamma^2=.4$ ).

Table 1. Probability of error for DS/SSMA systems with Rician nonselective fading ( $N=31, \gamma^2=.1$ ).

$E_b/N_0$	K=2			K=3			K=4		
	$\bar{P}_{e,1}^G$	$\bar{P}_{e,1}^{(i)}$	$\bar{P}_{e,1}^{(ii)}$	$\bar{P}_{e,1}^G$	$\bar{P}_{e,1}^{(i)}$	$\bar{P}_{e,1}^{(ii)}$	$\bar{P}_{e,1}^G$	$\bar{P}_{e,1}^{(i)}$	$\bar{P}_{e,1}^{(ii)}$
6	1.04	1.04	1.04	1.25	1.26	1.26	1.53	1.54	1.54
8	3.83	3.86	3.86	5.27	5.37	5.35	0.73	0.75	0.74
10	1.36	1.40	1.39	2.23	2.34	2.31	3.58	3.80	3.76
12	5.18	5.43	5.37	1.02	1.12	1.10	1.93	2.16	2.11
14	2.26	2.45	2.40	5.37	6.25	6.05	1.18	1.39	1.35
16	1.17	1.32	1.28	3.29	4.04	3.86	0.82	1.02	0.97

Table 2. Probability of error for DS/SSMA systems with different chip waveforms and Rician nonselective fading ( $K=3, N=31$ ).

$E_b/N_0$ (dB)	$\gamma^2=.01$				$\gamma^2=.1$			
	rect		sine		rect		sine	
	$\bar{P}_{e,1}^G$	$\bar{P}_{e,1}^{(i)}$	$\bar{P}_{e,1}^G$	$\bar{P}_{e,1}^{(i)}$	$\bar{P}_{e,1}^G$	$\bar{P}_{e,1}^{(i)}$	$\bar{P}_{e,1}^G$	$\bar{P}_{e,1}^{(i)}$
6	5.19	5.25	4.92	4.99	1.25	1.26	1.21	1.22
8	1.06	1.11	0.95	1.02	5.27	5.37	4.97	5.09
10	1.52	1.78	1.24	1.61	2.23	2.34	2.04	2.17
12	1.70	2.56	1.20	2.41	1.02	1.12	0.91	1.03
14	1.80	4.07	1.05	4.28	5.37	6.25	4.63	5.67
16	1.23	0.83	1.03	1.00	3.29	4.04	2.76	3.66

Table 3. Probability of error for a DS/SSMA system with Rayleigh nonselective fading ( $K=3$ ,  $N=31$ ).

$\bar{E}_b/N_0$	$\bar{\gamma}^2=.01$			$\bar{\gamma}^2=.1$			$\bar{\gamma}^2=.2$					
	$\bar{P}_{e,1}^G$	$\bar{P}_{e,1}^{(i)}$	$\bar{P}_{e,1}^{(ii)}$	$\bar{P}_{e,1}^G$	$\bar{P}_{e,1}^{(i)}$	$\bar{P}_{e,1}^{(ii)}$	$\bar{P}_{e,1}^G$	$\bar{P}_{e,1}^{(i)}$	$\bar{P}_{e,1}^{(ii)}$			
10	6.42	6.43	6.43	$(\times 10^{-2})$	6.47	6.51	6.51	$(\times 10^{-2})$	6.53	6.60	6.60	$(\times 10^{-2})$
20	2.35	2.34	2.34	$(\times 10^{-2})$	2.55	2.43	2.43	$(\times 10^{-2})$	2.74	2.53	2.53	$(\times 10^{-2})$
30	0.85	0.78	0.78	$(\times 10^{-2})$	1.34	0.87	0.87	$(\times 10^{-2})$	1.72	0.98	0.98	$(\times 10^{-2})$
40	4.37	2.59	2.59	$(\times 10^{-3})$	1.14	0.35	0.35	$(\times 10^{-2})$	1.56	0.46	0.46	$(\times 10^{-2})$
50	3.70	0.89	0.89	$(\times 10^{-3})$	11.2	1.83	1.83	$(\times 10^{-3})$	15.6	2.87	2.87	$(\times 10^{-3})$
$\infty$	36.2	1.07	1.07	$(\times 10^{-4})$	11.2	1.05	1.05	$(\times 10^{-3})$	15.6	2.08	2.09	$(\times 10^{-3})$

Table 4. Probability of error for a DS/SSMA system with frequency-selective fading ( $K=3$ ,  $\bar{\gamma}^2=.4$ ).

$E_b/N_0$ (dB)	N=31			N=127				
	$\bar{P}_{e,1}^G$	$\bar{P}_{e,1}^{(i)}$	$\bar{P}_{e,1}^{(ii)}$	$\bar{P}_{e,1}^G$	$\bar{P}_{e,1}^{(i)}$	$\bar{P}_{e,1}^{(ii)}$		
6	6.34	6.40	6.40	$(\times 10^{-3})$	3.20	3.20	3.20	$(\times 10^{-3})$
8	1.57	1.62	1.62	$(\times 10^{-3})$	3.78	3.82	3.82	$(\times 10^{-4})$
10	3.10	3.42	3.41	$(\times 10^{-4})$	1.83	1.97	1.97	$(\times 10^{-5})$
12	5.54	6.97	6.95	$(\times 10^{-5})$	3.31	3.89	3.89	$(\times 10^{-7})$
14	1.05	1.61	1.59	$(\times 10^{-5})$	1.91	3.22	3.20	$(\times 10^{-9})$
16	2.47	4.75	4.73	$(\times 10^{-6})$	0.44	1.02	1.01	$(\times 10^{-10})$

### Figure Captions

- Figure 1. Probability of error for a DS/SSMA system with Rician nonselective fading ( $K=3$ ,  $N=31$ , and  $\gamma^2=.01$ ,  $.05$ ,  $.1$ ,  $.2$ , and  $.4$ )
- Figure 2. Probability of error for a DS/SSMA system with frequency-selective fading ( $N=31$ ,  $\gamma^2=.4$ , and  $K=2,3$ , and  $4$ ).
- Figure 3. Probability of error for a DS/SSMA system with frequency-selective fading ( $K=3$ ,  $N=31$ , and  $\gamma^2=0.$ ,  $.1$ ,  $.2$ ,  $.4$ , and  $.6$ )

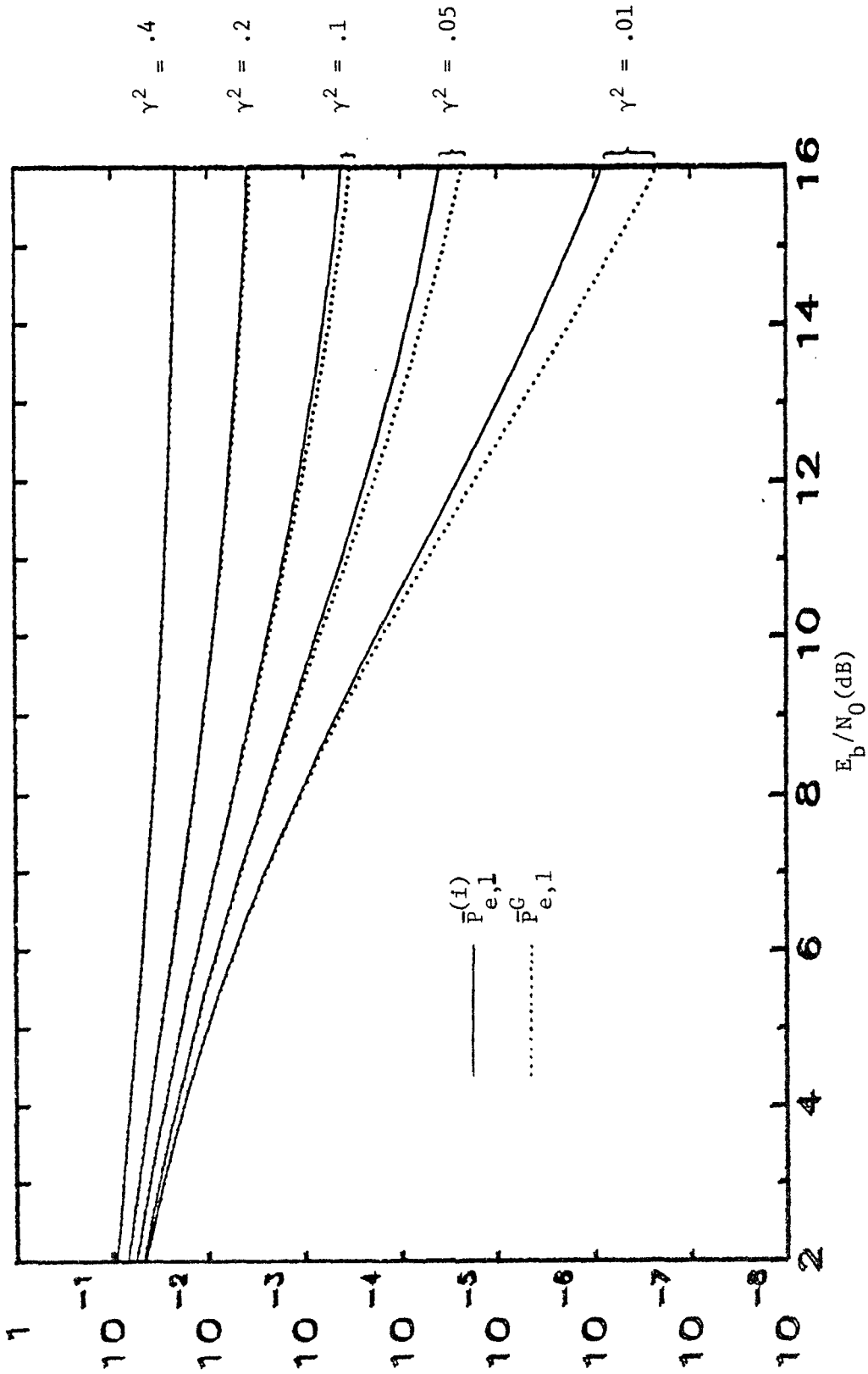


Figure 1. Probability of error for a DS/SSMA system with Rician nonselective fading ( $K = 3$ ,  $N = 31$ , and  $\gamma^2 = .01, .05, .1, .2$ , and  $.4$ )

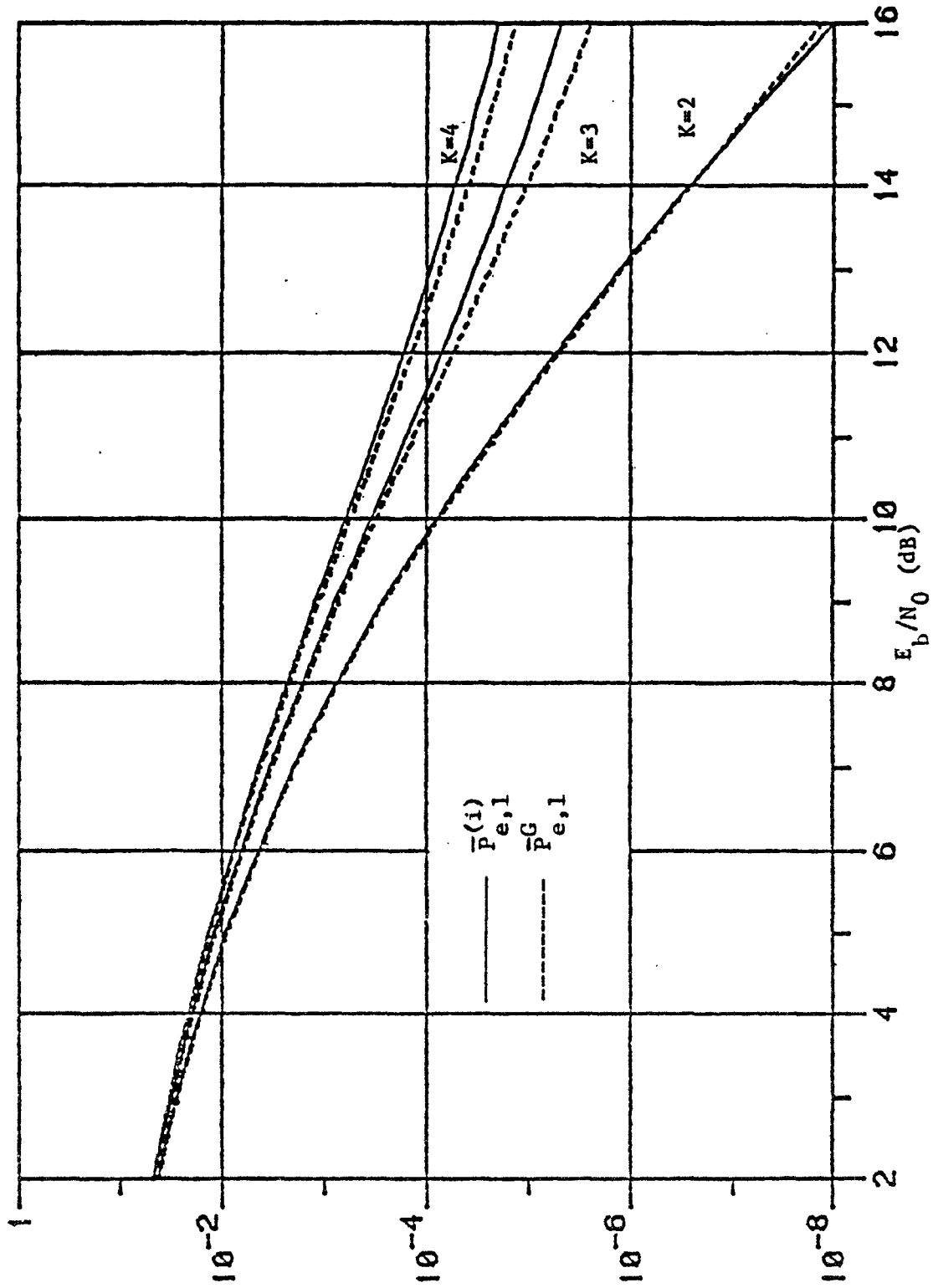


Figure 2. Probability of error for a DS/SSMA system with frequency-selective fading ( $N = 31$ ,  $\gamma^2 = .4$ , and  $K = 2, 3$ , and 4).

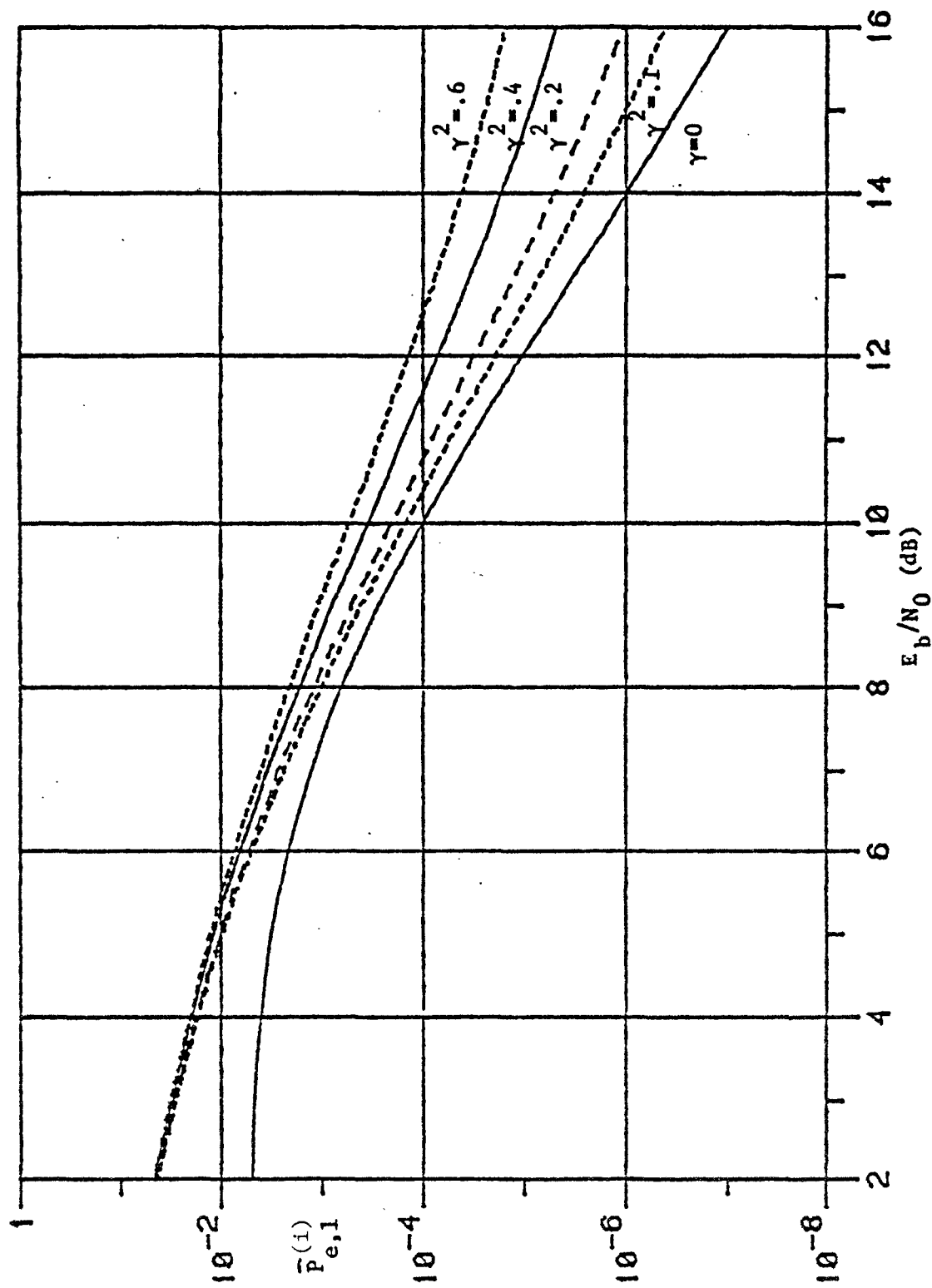


Figure 3. Probability of error for a DS/SSMA system with frequency-selective fading  
 ( $K = 3$ ,  $N = 31$ , and  $\gamma^2 = 0.1, .2, .4, \text{ and } .6$ )